

STM images of a superconducting Cu-O plane and the corresponding tunneling spectrum in $\text{Bi}_2\text{Sr}_2\text{CaCu}_2\text{O}_{8+\delta}$

M. Oda, C. Manabe, and M. Ido

Department of Physics, Faculty of Science, Hokkaido University, Sapporo 060, Japan

(Received 6 July 1995)

Clear atomic images of $\text{Bi}_2\text{Sr}_2\text{CaCu}_2\text{O}_{8+\delta}$ cleaved surfaces have been observed at $T=6$ and 300 K by scanning tunneling microscopy (STM). The atomic images taken for bias voltages much lower than the Bi-O plane semiconducting gap $E_g \sim 100$ meV, corresponding to the Cu-O plane, indicate that the conduction electrons exist mainly in the Cu $3d_{x^2-y^2}$ and O $2p_\sigma$ orbitals. Tunneling spectra have been also measured in the same processes as in the Cu-O plane STM image observations at $T=6$ K. The low-temperature spectra are in good agreement with that in a d -wave superconductor with an anisotropic Fermi surface on which the normal density of states $N(\mathbf{k}_F)$ is largest (N_{\max}) for the maximum gap directions and decreases to $\sim N_{\max}/2$ for the node directions. This, combined with the result on the $N(\mathbf{k}_F)$ anisotropy in photoemission experiments, is consistent with a $d_{x^2-y^2}$ superconducting gap.

For understanding the pairing mechanism responsible for high- T_c superconductivity, it is of great interest to elucidate the symmetry of the order parameter. For this reason, the low-temperature ($T \ll T_c$) electronic energy spectra in high- T_c cuprates have been extensively studied in various kinds of experiments.¹⁻⁵ Tunneling spectroscopy is a powerful tool for the study of energy spectrum near the Fermi level on account of its high energy resolution. Earlier tunneling experiments on high- T_c cuprates, including spectroscopy STS by scanning tunneling microscopy (STM), suggested the existence of a finite gap over the entire Fermi surface, that is, an s -wave superconducting gap.^{6,7} On the other hand, Barbiellini *et al.* have recently reported that their STS data in $\text{Bi}_2\text{Sr}_2\text{CaCu}_2\text{O}_{8+\delta}$ (Bi2212) fit well to a quasiparticle spectrum calculated for a d -wave superconductor.⁴ Furthermore, Manabe *et al.* have shown tunneling spectra suggesting the existence of nodes in the Bi2212 superconducting gap, together with observations of the clear atomic images by STM.⁵ In tunneling experiments, the specimen surface is required to be perfect on an atomic scale because of its short sampling depth. Observation of a clear atomic image by STM guarantees that the specimen surface is of high quality on the atomic scale. Therefore, STS should be performed in the same processes as in observations of clear atomic images.

In high- T_c cuprates Bi2212 has been most frequently subjected to STM-STS studies, because clean surfaces can be obtained by cleaving. This compound is composed of ~ 15 Å half-cells along the c axis in which an insulating Ca plane at the center is sandwiched in turn by two metallic (superconducting) Cu-O planes, by two insulating Sr-O planes and by two semiconducting Bi-O planes. The semiconducting gap E_g of the Bi-O plane is typically ~ 100 meV and slightly reduced with oxygen content.^{8,9} The Bi2212 crystal is cleaved between two Bi-O planes, which are, respectively, located at the top and bottom of the half cells; therefore, in STM experiments on the cleaved surfaces of Bi2212, the top atomic plane closest to the STM tip is the Bi-O plane, the second the Sr-O plane and the third the Cu-O plane, as schematically shown in Fig. 1. The electronic density of states in the Bi-O plane is considered to be zero in the energy range of

$-E_g < E < E_g$. This, together with the fact that the Sr-O plane is insulating, means that tunneling of electrons occurs from the metallic Cu-O plane when the bias voltage V_0 is lower than E_g/e and the STM tip is very close to the specimen surface. Therefore, the STM images of the Bi2212 cleaved surfaces taken for $V_0 \ll E_g/e$ are expected to be of the Cu-O plane. On the other hand, for $V_0 \gg E_g/e$, tunneling of electrons occurs mainly from the Bi-O plane, the atomic plane closest to the STM tip. Indeed, the STM images taken for $V_0 \gg E_g/e$ agree well with the Bi-atom arrangement with a significant modulation structure, and the tunneling spectra measured in the same processes as in the STM image observations are semiconducting, as shown by Kitazawa *et al.*⁶ and by Xiang *et al.*¹⁰

In this paper, we report that clear STM images of the Cu-O plane were observed on the Bi2212 cleaved surfaces by using bias voltages much lower than E_g/e , and that tunneling spectra, measured while observing the Cu-O plane STM images at $T=6$ K, are explained very well in terms of small pair-breaking effects in a $d_{x^2-y^2}$ superconducting state.

The Bi2212 single crystals used were grown in magnesia crucibles by a flux method. No impurity phases for the grown crystals were detected by x-ray diffraction experiments. The grown crystals exhibited a sharp superconducting diamagnetic transition at $T_c=82$ K. Specimens of size $\sim 3 \times 3 \times 1$ mm³ were selected from a batch of single crystals for the STM-STS measurements.

A cryogenic STM-STS system (Olympus LTSTM-300) was used in the present experiments. A Pt-Ir alloy was used for the STM tip. The specimens were cleaved in air imme-

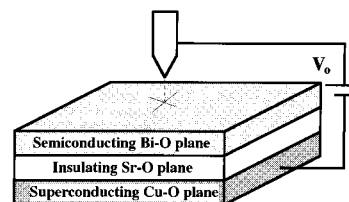


FIG. 1. Schematic of the STM image observation on the Bi2212 cleaved surface.

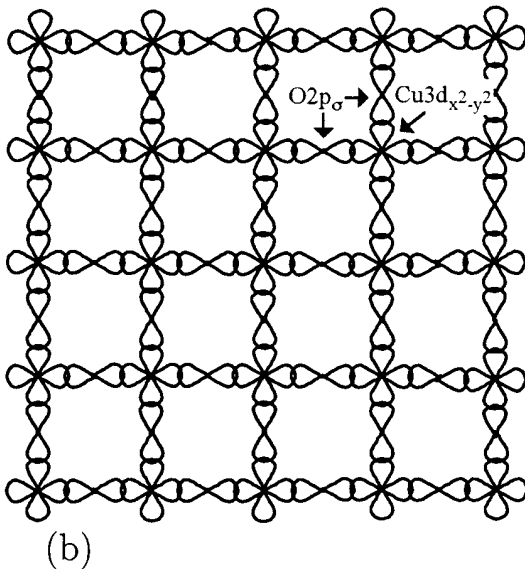
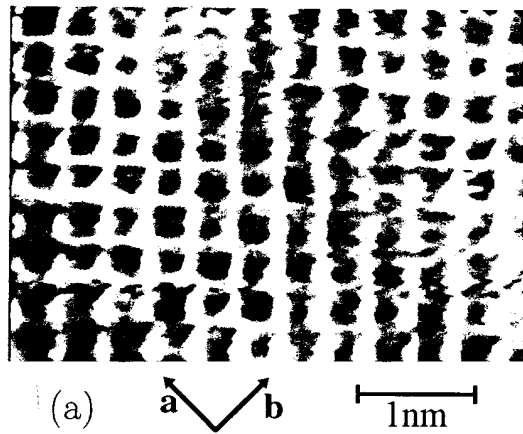


FIG. 2. (a) Low-bias STM image of the Bi2212 cleaved surface taken for $V_0=20$ mV, $I_0=1$ nA and $T=6$ K. (b) Schematic of two-dimensional arrays of the Cu $3d_{x^2-y^2}$ and O $2p_{\sigma}$ orbitals.

diately before being mounted in the STM sample chamber with a vacuum higher than 1×10^{-6} Torr and cooled down to $T=6$ K. The STM image observations were performed in the constant distance mode; keeping the distance from the specimen surface constant under a bias voltage V_0 , the STM tip is scanning along the surface. In the course of scanning, the tunneling current was recorded and displayed as a function of the tip position. In the STS experiments, an STM image was first taken, and the position for STS was determined on the STM image. In the following STM image observation, scanning of the STM tip was interrupted for 20 seconds at the position indicated for STS, and during this period I - V and dI/dV - V curves were measured. Thus, tunneling spectra were obtained in the same processes as in STM image observations.

An STM image of the Bi2212 cleaved surface at $T=6$ K is shown in Fig. 2(a). This STM image was taken under a bias voltage $V_0=20$ mV and a tip-surface distance giving tunneling current $I_0=1$ nA at the initial position. Similar STM images were also observed for $V_0=10$ mV and 50 mV, although for $V_0=50$ mV the images were not so clear as for $V_0=20$ mV. In Fig. 2(a) atomic corrugations are seen along ~ 4 Å perimeters of squares. The weak modulation structure

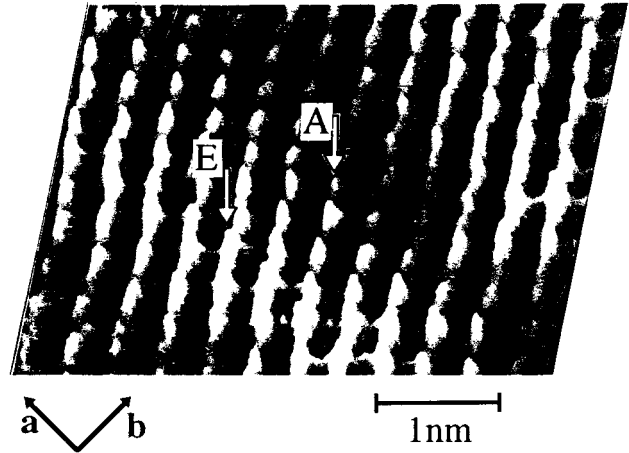


FIG. 3. STM image of another area of the same specimen under the same conditions as in Fig. 2(a).

of the ~ 25 Å period along the diagonal line direction (b axis) of the squares can be confirmed in low-bias STM images for a slightly larger area (Fig. 3).⁵ STS at room temperature revealed the semiconducting gap of the Bi-O plane $E_g \sim 100$ meV for the present specimens. This value of E_g is comparable to the result reported by Shih *et al.*⁸ and by Hasegawa and Kitazawa.⁹ It should be noted here that the bias voltage ($V_0=20$ mV) used for the STM image observation in Fig. 2(a) was much lower than E_g/e . In this case the density of states in the Bi-O plane is considered to be zero in an energy range from the Fermi level E_F to E_F+eV_0 . This, together with the fact that both the Sr-O and Ca planes are insulating, means that the tunneling current for $V_0 \ll E_g/e$ comes mainly from the metallic Cu-O plane, as mentioned above. The corresponding STM image, shown in Fig. 2(a), is therefore of the Cu-O plane.

In the Cu-O plane, the Cu atoms form a square-lattice and the O atoms are located at the midway between two adjacent Cu atoms. The ~ 4 Å perimeter of the squares formed by the atomic corrugations is comparable to the Cu-O-Cu distance, and it is clear from the direction of the weak modulation structure in Figs. 2(a) and 3 that the diagonal lines of the squares are along the directions 45° from the Cu-O bond directions. Such atomic corrugations in the low bias STM images agree well with the two-dimensional arrays of the Cu $3d_{x^2-y^2}$ and O $2p_{\sigma}$ orbitals as schematically shown in Fig. 2(b). This result indicates that the conduction electrons, responsible for tunneling, exist in a band arising mainly from these orbitals.

Similar STM images were also observed in another specimens for $V_0=10$ and 20 mV ($\ll E_g/e$) at $T=6$ K and 300 K. On the other hand, STM images taken at $V_0=500$ mV, much higher than E_g/e , were rather different from the low bias STM images; the atomic corrugations of high bias STM images are consistent with the Bi-atom arrangement which has a significant modulation structure along the b axis. High-resolution electron microscopy has revealed that the modulation structure in the Cu-O plane is much weaker than in the Bi-O plane,¹¹ as in Figs. 2(a) and 3. This result strongly supports the contention that the low bias STM images of the Bi2212 cleaved surfaces are of the Cu-O plane, as well.

Figure 3 shows an STM image of another area of the

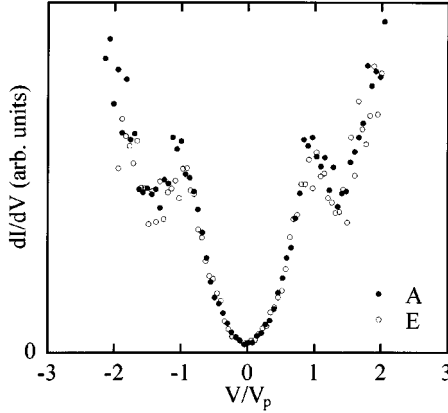


FIG. 4. dI/dV - V curves measured at positions A and E on the STM image shown in Fig. 3. The bias-voltages V are normalized with V_p , which is 33 and 35 mV for positions A and E, respectively.

same specimen taken under the same conditions as in Fig. 2(a). The weak modulation structure along the b axis can be seen more clearly in this figure. Dependences of differential conductance dI/dV on bias-voltage V are shown in Fig. 4, which were measured at positions A and E in relatively dark and bright regions of the weak modulation structure in Fig. 3. The conductance dI/dV is very small at $V=0$, and exhibits peaks at $|V|=V_p$. These features agree qualitatively with expectations for a superconducting gap.

Low-temperature tunneling spectra on the Bi2212 cleaved surfaces have been measured in the same processes as in STM image observations by Kitazawa *et al.*⁶ and by Xiang *et al.*¹⁰ The STM images were of the Bi-O plane and the spectra were semiconducting, because their STM-STs experiments were carried out in the conditions in which the electron tunneling occurred only from the Bi-O plane closest to the STM tip, that is, for bias voltages much higher than E_g/e and for long tip-surface distances. In our STM-STs experiments, however, the STM images of the Cu-O plane were observed by using bias voltages much lower than E_g/e , and the superconducting spectra could therefore be obtained in the same processes as in the STM image observations.

Almost the same dI/dV - V curves were also observed at other positions, although the bias voltages V_p exhibiting dI/dV peaks were slightly different from position to position within $\pm 5\%$ of the average. The magnitude of energy gap defined by $2eV_p$, hereafter referred as the maximum energy gap $2\Delta_{\max}$, was almost the same as the results reported for the Bi2212 cleaved surface by many groups^{4,6,12,13} and also the result reported for the lateral surface.⁷ At high voltages of $|V|\geq 60$ mV, the dI/dV - V curve turned upward and was roughly consistent with a straight line, as seen in Fig. 4; it seems that for $|V|\geq 60$ mV a linearly dependent background superposes on the superconducting spectrum which will be saturated to the normal state value at high voltages. Although the origin of the background has not been clarified yet, it might arise from the semiconducting Bi-O plane,⁵ or might be due to some influence of the STM tip to the specimen.¹⁴ Here, the linearly dependent background for $|V|\geq 60$ mV was subtracted from the dI/dV - V curve observed at position A as the data became roughly constant at high voltages (Fig. 5). The tunneling spectrum thus obtained is consistent with

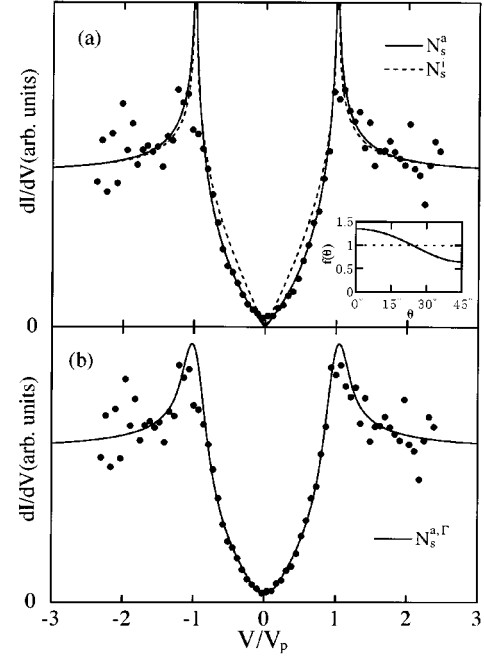


FIG. 5. Comparisons between the tunneling spectrum for position A and the quasiparticle spectra in d -wave superconductors. The calculated spectra $N_s^i(E)$ is for a system with isotropic Fermi surface, and $N_s^a(E)$ is for a system with an anisotropic Fermi surface on which the normal density of states $N(\mathbf{k}_F)$ is largest (N_{\max}) for the maximum gap directions and decreases to $\sim N_{\max}/2$ for the node directions. The calculated spectrum $N_s^{a,\Gamma}(E)$ involves a small broadening effect ($\Gamma \sim 3$ meV) in $N_s^a(E)$. The inset shows the weighting function $f(\theta)$ used in the calculation of $N_s^a(E)$.

that in a d -wave superconductor, as described below in detail.

In a two-dimensional d -wave superconductor with line nodes, the quasiparticle spectrum $N_s^l(E)$ is given by the following equation when the system has an isotropic Fermi surface:

$$N_s^l(E)/N_n = \text{Re} \int_0^{2\pi} \frac{d\theta}{2\pi} \frac{E}{\sqrt{E^2 - \Delta(\theta)^2}}, \quad (1)$$

where N_n is the normal density of states at the Fermi level and $\Delta(\theta)$ is the order parameter written $\Delta_{\max} \cos(2\theta)$.¹⁵⁻¹⁷ Qualitative behaviors of the observed spectrum are very similar to those of the calculated spectrum [the broken line in Fig. 5(a)]. However, these spectra do not agree quantitatively in the following two points: (i) a small finite dI/dV value at $V=0$ and suppressions of the dI/dV peaks at $|V| \sim V_p$, and (ii) downward deviations of the dI/dV data from the calculated spectrum at low voltages except for $V \sim 0$. The latter behavior is expected in a d -wave superconductor with an anisotropic Fermi surface on which the normal density of states $N(\mathbf{k}_F)$ is largest (N_{\max}) for the maximum gap directions and less (N_{\min}) than the average over the entire Fermi surface for the node directions. Indeed, the quasiparticle spectrum $N_s^a(E)$ calculated for the $N(\mathbf{k}_F)$ anisotropy factor $N_{\max}/N_{\min} = 2.1$ reproduces well the dI/dV data deviating downward from $N_s^l(E)$, as shown in Fig. 5(a). In the calculated spectrum $N_s^a(E)$, the $N(\mathbf{k}_F)$ anisotropy is taken into account by introducing the weighting function $f(\theta)$ [the inset in Fig. 5(a)] into the integral of Eq. (1):

$$N_s^a(E)/N_n = \text{Re} \int_0^{2\pi} \frac{f(\theta)d\theta}{2\pi} \frac{E}{\sqrt{E^2 - \Delta(\theta)^2}}. \quad (2)$$

Angle-resolved photoemission experiments in Bi2212 have shown an extended region of flat bands close to the Fermi level E_F around the Cu-O bond directions (the k_x and k_y axes).¹⁸ Furthermore, it has recently been reported in STS experiments by Renner and Fischer that Bi2212 crystals with $T_c \sim 92$ K can be described as a d -wave superconductor in which the energy band in the normal state has a van Hove singularity near $E = E_F$.^{4,14} On the basis of the results on the photoemission experiments, the normal density of states $N(\mathbf{k}_F)$ in Bi2212 is largest around the k_x and k_y axes and less than the average over the entire Fermi surface around the directions 45° (the 45° off-axes) from the k_x and k_y axes. Such a $N(\mathbf{k}_F)$ anisotropy is in qualitative agreement with the results from band calculations for the Cu-O plane of this system.¹⁹ Although the magnitude of $N(\mathbf{k}_F)$ anisotropy in Bi2212 depends on the location of E_F in the energy band or the hole concentration of the crystal, the qualitative tendency in the angular dependence of $N(\mathbf{k}_F)$ will not change with the hole concentration. It should be noted that our STS data fit well to the theoretical curve in a d -wave superconductor in which $N(\mathbf{k}_F)$ is largest for the maximum gap directions and smallest for the node directions. This, combined with the result for the Bi2212 $N(\mathbf{k}_F)$ anisotropy in the photoemission experiments, indicates that the maximum gap occurs along the k_x and k_y axes, while the node occurs along the 45° off-axes. Therefore, our STS data are consistent with a $d_{x^2-y^2}$ superconducting gap.

Kane *et al.*²⁰ have studied gap anisotropy within the k_x - k_y plane in tunneling experiments on the lateral surface of Bi2212 and reported the maximum gap in the 45° off-axes, contrary to the present result. On the other hand, Tanaka *et al.* have recently proposed a model that electron tunneling occurs mainly from the O $2p_\sigma$ orbitals on the surface Cu-O plane and reported that based on the model the observed gap anisotropy is consistent with a $d_{x^2-y^2}$ gap.²¹ Angle-resolved photoemission and Raman scattering experiments in Bi2212 have also shown a significant gap anisotropy consistent with $d_{x^2-y^2}$ symmetry.^{22,23}

Recent angle-resolved photoemission experiments have reported an extended s -wave symmetry in which a small

finite gap Δ_s exists for the 45° off-axis directions and nodes are located at both sides of these axes.²⁴ In this case, dI/dV peaks or humps at $|V| \sim \Delta_s/e$ are expected in the tunneling spectrum of Bi2212. However, such a subgap structure was not observed in the present data (Figs. 4 and 5).

The solid line in Fig. 5(b) involves a small broadening effect in the quasiparticle spectrum $N_s^a(E)$ given by the Gaussian distribution function:

$$N_s^{a,\Gamma}(E_i) = \sum_j N_s^a(E_j) \frac{\exp[-(E_i - E_j)^2/2\Gamma^2]}{\sqrt{2\pi}\Gamma} \Delta E, \quad (3)$$

where the deviation $\Gamma = 0.1\Delta_{\max} \sim 3$ meV and $\Delta E \equiv E_{i+1} - E_i \ll \Delta_{\max}$. As seen in Fig. 5(b), the broadening of the spectrum can explain the small finite zero-bias dI/dV and the suppressions of the dI/dV peaks at $|V| \sim V_p$, due to some pair-breaking effects in a superconductor with line nodes. The fit of the calculated spectrum $N_s^{a,\Gamma}(E)$ to our dI/dV data gives $N_s^{a,\Gamma}(0)/N_n \sim 0.06$, indicating the spectral weight at E_F in the superconducting state $\sim 6\%$ of the value in the normal state. The existence of residual spectral weight at E_F in the Bi2212 superconducting state has also been reported in NMR experiments on spin excitations by Tanigawa and Mitzi²⁵ and by Ishida *et al.*²⁶ The residual spectral weight in the NMR experiments is 10–20 % of the normal spectral weight, a little larger than that in our STS studies.

In conclusion, clear STM images of the Cu-O plane were observed on the Bi2212 cleaved surfaces for $V_0 \ll E_g/e$, and tunneling spectra were also measured in the same processes as in the STM image observations at $T = 6$ K. It should be noted again that the lowest bias voltage used for STM image observations of the superconducting Cu-O plane was also smaller than the maximum gap ($V_0 \sim \Delta_{\max}/3e$), meaning that superconducting quasiparticle excitations exist even in a low energy region at least below $E \sim \Delta_{\max}/3$. Furthermore, our STS data can be explained very well in terms of small pair-breaking effects in a $d_{x^2-y^2}$ superconducting state.

The authors would like to thank Professor R. Aoki, Professor K. Kitazawa, and Professor M. Sato for valuable discussions. This work was supported in part by a Grant-in Aid for Scientific Research from the Ministry of Education, Science and Culture, Japan.

¹W. N. Hardy *et al.*, Phys. Rev. Lett. **70**, 3999 (1993).

²N. Momono *et al.*, Physica C **233**, 395 (1994).

³K. A. Moler *et al.*, Phys. Rev. Lett. **73**, 2744 (1994).

⁴B. Barbiellini *et al.*, Physica C **220**, 55 (1994).

⁵C. Manabe *et al.*, Physica C **235-240**, 797 (1994).

⁶K. Kitazawa *et al.*, Physica C **209**, 23 (1993).

⁷K. Ichimura and K. Nomura, Solid State Commun. **82**, 171 (1992).

⁸C. K. Shih *et al.*, Phys. Rev. B **43**, 7913 (1991).

⁹T. Hasegawa and K. Kitazawa, Jpn. J. Appl. Phys. **29**, 434 (1990).

¹⁰Jin-Xiang Liu *et al.*, Phys. Rev. Lett. **67**, 2195 (1991).

¹¹Y. Matsui *et al.*, Jpn. J. Appl. Phys. **27**, 372 (1988).

¹²A. Chang *et al.*, Phys. Rev. B **46**, 5692 (1992).

¹³Jie Liu *et al.*, Phys. Rev. B **49**, 6234 (1994).

¹⁴Ch. Renner and Ø. Fischer, Phys. Rev. B **51**, 9208 (1995).

¹⁵H. Won and K. Maki, Phys. Rev. B **49**, 1397 (1994).

¹⁶P. Monthoux *et al.*, Phys. Rev. B **46**, 14 803 (1992).

¹⁷F. J. Ohkawa, J. Phys. Soc. Jpn. **56**, 2267 (1987).

¹⁸D. Dessau *et al.*, Phys. Rev. Lett. **71**, 2781 (1993).

¹⁹S. Massidda *et al.*, Physica C **152**, 251 (1988).

²⁰J. Kane *et al.*, Phys. Rev. Lett. **72**, 128 (1994).

²¹S. Tanaka *et al.*, J. Phys. Soc. Jpn. **64**, 1476 (1995).

²²Z.-X. Shen *et al.*, Phys. Rev. Lett. **70**, 1553 (1993).

²³T. P. Devereaux *et al.*, Phys. Rev. Lett. **72**, 396 (1994).

²⁴H. Ding *et al.*, Phys. Rev. Lett. **74**, 2784 (1995).

²⁵M. Tanigawa and D. B. Mitzi, Phys. Rev. Lett. **73**, 1287 (1994).

²⁶K. Ishida *et al.*, J. Phys. Soc. Jpn. **63**, 1104 (1994).